Hydrodynamic Mobility of an Optically Trapped Colloidal Particle near Fluid-Fluid Interfaces

G. M. Wang,[1] R. Prabhakar,[2] and E. M. Sevick[1,*]

[1]*Research School of Chemistry, The Australian National University, Canberra ACT 0200, Australia*
[2]*Department of Mechanical & Aerospace Engineering, Monash University Clayton VIC 3800, Australia*

(Received 7 August 2009; published 8 December 2009)

Using optical tweezers, we measure the anisotropic hydrodynamic mobility of a colloidal particle by tracking its thermal motion in an optical trap located near fluid-fluid interfaces, namely, liquid-vapor and liquid-liquid interfaces. The method requires no controlled fluid flow, is independent of conservative interactions between particle and interface, and resolves distance dependent friction to within a fraction of the particle radius. Near the liquid-vapor interface, the friction decreases below that in the bulk, corresponding to predictions of a "perfect-slip" surface.

DOI: 10.1103/PhysRevLett.103.248303 PACS numbers: 82.70.Dd, 66.20.Ej, 68.03.−g, 68.05.−n

The aim of microfluidics is to miniaturize reaction vessels and their connecting conduits to "lab on a chip" dimensions. However, this magnifies the influence of bounding walls on the microflow. The drag force on a particle entrained in these microfluidic flows is larger than the particle's drag in a bulk fluid. This is due to the hydrodynamic interactions between colloid and surrounding solvent molecules being altered by the nearby solid surface. These microvessel boundaries need not be solid surfaces, but can also be soft surfaces, such as in vesicle membranes, or an immiscible fluid that forms impenetrable boundaries. Fluid mechanists have derived theoretical predictions of how the particle friction becomes anisotropic and dependent upon distance from a surface that is governed by various boundary conditions [1–5]. However, experimental measures of particle friction near a single surface are comparatively few and exist only near solid surfaces.

The hydrodynamics near solid surfaces was thought to be understood in the 19th century; however, recent experimental reports of fluid "slip" (or nonzero fluid velocity) at hydrophobic solid surfaces have spurred several recent investigations (for a review, see [6,7]). Such slip corresponds to a decreased particle friction near a solid surface, and decreased energy dissipation—and, consequently, such slip surfaces are of considerable interest in energy savings. There has been significant debate about the microscopic mechanisms which cause slip. There is some consensus that the slip interpretation of some experiments might be complicated by the presence of an adsorbed gas layer near the solid surface, which could give rise to an apparent "slip." Indeed, a recent strategy for producing drag-reducing solid surfaces focussed upon the capture and retention an adjacent gas layer with a fine-structured superhydrophobic surface [8].

In this Letter, we report the first experimental measurements of the hydrodynamic anisotropic friction of a colloidal particle as a function of distance from fluid-fluid interfaces, including a gas-liquid interface that does not support a stress. Our experimental method, optical tweezers (OT), uses light to localize a transparent colloidal particle near the bounding interfaces of a thin water film (Fig. 1). The particle's thermal motion in the optical trap depends sensitively upon the nearby surface and our precise measurements of these particle fluctuations provide us with a quantitative measure of the particle's friction and how it varies with distance and direction from the surface. This method is "passive" in the sense that the particle's friction is measured in a quiescent fluid without external imposition of either a flow or bulk motion of the particle.

The hydrodynamic friction or Stokes' drag on a particle of radius a in a bulk fluid of viscosity η is $\xi_0 = 6\pi\eta a$, which is inversely related to the diffusivity $D_0 = k_B T/\xi_0$ or mobility of the particle, $\mu_0 = 1/\xi_0$ (here we use mo-

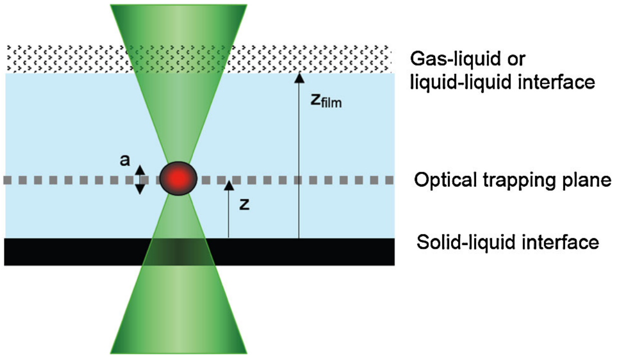

FIG. 1 (color online). An illustration of the optical tweezers method to determine the anisotropic mobility of a colloidal particle confined to an optical trap near an interface. When generated with a high numerical aperture lens and a light beam with Gaussian intensity (TEM_{00}), the optical trap provides a harmonic potential which tightly confines the colloid's diffusive motion to a two-dimensional trapping (focal) plane, localizing the motion about the focal point. Analysis of the particle fluctuations in the frequency domain yields values of z-dependent diffusivity parallel to the interface, (or $D_{\parallel}$), in the vicinity of the lower liquid-solid interface or an upper liquid-vapor or liquid-liquid interface.

bility and diffusivity interchangeably). When a particle's center is located a small distance z from a surface, where z/a can be on the order of a few particle radii, the diffusivity becomes anisotropic, with its components parallel and perpendicular to the surface, $D_\parallel$ and $D_\perp$, differing considerably in value from the isotropic bulk diffusivity, D_0. An exact hydrodynamic formulation of $D_\perp/D_0$ for a particle near a solid surface with no-slip boundary conditions was given famously by Brenner [1], replacing the lubrication approximation attributed to GI Taylor, and complementing Faxen's Law [9] for $D_\parallel/D_0$ near no-slip solid surfaces. These predictions, as well as more recent ones for different boundary conditions, follow the form

$$D_{\parallel,\perp}/D_0 = 1 + \sum_i g_i^{\parallel,\perp}(a/z)^i,$$

where the closed-form expressions for the coefficients in the power series $g_i^{\parallel,\perp}$ depend upon prescribed boundary conditions [1,3–5,9]. Further, Lauga and Squires [4] constructed predictions for $D_\parallel/D_0$ near solid surfaces using a boundary condition that was characterized by a parameter called the "slip length": variation of the slip length parameter from zero to infinity provides formulae that recover the limiting, classical cases of no-slip and perfect-slip boundary conditions.

For a shear-stress free surface, where there is perfect slip, it is predicted [2,3] that the friction of a particle moving parallel to the surface is *reduced* as z/a approaches 1. In contrast, particle friction near a no-slip surface is *enhanced*. Indeed, between the vapor and solid interfaces, $D_\parallel/D_0$ is predicted by theory to vary from about 3/2 to 1/2. The leading order term in the asymptotic expansion for $D_\parallel/D_0$ is altered dramatically with boundary condition, changing sign from $g_1^\parallel = -9/16$ for the no-slip to $g_1^\parallel = +3/8$ for the perfect-slip condition. In contrast, for $D_\perp/D_0$, $g_1^\perp$ is less sensitive to boundary condition, changing from $-9/8$ for no-slip to $-3/4$ for perfect slip. Thus, a measurement of $D_\parallel/D_0$ more sensitively detects the interface condition than measures of $D_\perp/D_0$. In what follows, we describe a high-resolution technique to measure $D_\parallel/D_0$ near interface, and further provide the first experimental evidence for decrease in parallel-friction near a gas-liquid interface, in an apparent measure of perfect slip.

Experimental measures of anisotropic mobility have been limited to near a solid surface, often with the aim to experimentally fit a slip parameter for hydrophobic surfaces. Most of the experiments record the thermal motion of a colloidal particle near a solid surface, using dynamic light scattering (DLS), particle tracking or fluorescence spectroscopy. Some investigate colloid mobility within fluid-filled slits of varying thickness h and report an isotropic diffusivity $D = \langle r^2(t)\rangle/2t$ averaged over small slit thicknesses [10,11], while others resolve parallel and perpendicular components of $\langle r^2(t)\rangle$ within fluid layers of thickness Δz located z from a solid surface [12], or between two parallel walls [13]. However, when close to the solid surface, $D_{\parallel,\perp}$ can vary strongly over a particle diameter, and as Δz is usually on the order of a particle radius or more, the experimental error in $D_{\parallel,\perp}(z)$ increases as the surface is approached. Moreover, z-dependent conservative interactions, such as long-ranged electrostatic interactions between the particle and surface, can bias diffusive trajectories and consequently, a fitting exercise is required to remove this bias from experimental data. Alternatively, long-ranged electrostatic interactions at a solid surface can be minimised with added salt; however, this is not an ideal remedy for fluid-fluid or membrane surfaces as this potentially changes the surface. Importantly, attempts to fit the experimental measures of colloidal Brownian motion to a slip length parameter are ambiguous due to this lack of resolution at close distances to the solid surface, where mobility varies most dramatically.

The use of OT to probe hydrodynamics at solid surfaces overcomes these experimental limitations. By tightly confining the particle's diffusive motion to a focal plane parallel to the flat surface, i.e., pinning the particle's z distance from the surface, the influence of long-ranged colloid-surface interactions is effectively removed in parallel-mobility measurement. The focused laser's intensity determines the tightness of the trap, which limits the particle's diffusive excursions from the focal point. Thus the range of diffusive motion can be adjusted to minimize the variation in z and the influence of long-ranged conservative interactions with the surface. In addition, the resolution in measured $D_{\parallel,\perp}(z)$ is also enhanced. The particle's motion at low frequencies details the "rattling" of the colloid within the confining optical trap; at high frequencies the hydrodynamic diffusivity can be probed, and at even higher frequencies, the effect of inertia can be explored [14]. Shaffer *et al.* [15] demonstrated the enhanced resolution of OT measurements of colloid mobility or friction near solid surfaces and showed a significant reduction in the experimental error in $D_{\parallel,\perp}(z)$ within a few particle diameters of the solid surface.

Here we report OT measurements of a colloid's hydrodynamic mobility/friction in a water layer bounded by a solid and a fluid-fluid interface, namely, an immiscible liquid-liquid interface or a liquid-gas interface. Our method pins a single colloidal particle to an x-y focal plane, located a distance z from an interface and confines the diffusive motion in the $x = \{x, y\}$ plane by a harmonic potential. The particle motion obeys the Langevin equation

$$\xi_\parallel \frac{dx}{dt} = -kx + f,$$

where $\xi_\parallel$ is the particle's anisotopic and z-dependent friction coefficient, k is the optical trapping constant, and f is a random force, characterized by a mean and variance of $\langle f(t)\rangle = 0$ and $\langle f(t)f(t')\rangle = 2k_BT\xi_\parallel\delta(t - t')$. A solution to the inertialess Langevin equation is

$$x(t) = x(0)\exp[-t/\tau_{\|}] + \frac{1}{\mu_{\|}}\int_0^t dt' \exp[-(t-t')/\tau_{\|}] f(t'),$$

where the characteristic time scale is $\tau_{\|} = \xi_{\|}/k$. The correlation function, $C(t)$, defined as $C(t) = \langle x(t)x(0)\rangle$, is $C(t) = \frac{k_B T}{k}\exp[-t/\tau_{\|}]$ by equipartition. The Fourier transform of the time correlation function $C(t)$ is referred to as the power spectrum density, $\mathrm{PSD}(\omega)$ and is

$$\mathrm{PSD}(\omega) = \langle | \tilde{x}(\omega) |^2 \rangle = \frac{2D_{\|}}{\tau_{\|}^{-2} + \omega^2}. \qquad (1)$$

We construct power spectral densities from the Fourier transform of experimentally sampled trajectories of an optically trapped colloid, $x(\omega)$, and fit eqn (1) to the data, determining $D_{\|}$ as a fitting parameter. For consistency, we also ensure that

$$\tau_{\|} \equiv \frac{\xi_{\|}}{k} = \frac{\langle x(0)^2 \rangle}{D_{\|}}.$$

We apply our OT technique to probe the mobility of a 5.08 μm-dia. silica particle in water in proximity to three different surfaces: a hydrophilic surface, an oil interface, and a vapor interface. These interfaces are created using a film of deionized, purified water, roughly 100 μm (up to 800 μm) thick and containing 100 silica particles, on a plasma-cleaned (hydrophilic) glass coverslip. One ml of mineral oil was added to the top of the water to create a film bounded by a hydrophilic solid and an immiscible liquid. To minimize evaporation during data recording, we sealed the vapor-exposed water films, with a second coverslip to create a liquid-vapor interface, and allowed the thin vapor and water films to equilibrate. Each of these samples were placed in the optical tweezers apparatus described in Wang *et al.* [16] The OT apparatus consists of a Nikon DIAPHOT 300 inverted microscope equipped with a 63× (NA = 0.75) LWD (Long Working Distance, up to 1.5 mm) objective lens and a 4 W infrared laser ($\lambda = 1064$ nm) isolated on an air-cushioned optical table. A servo-motor controls the z placement of the microscope stage to within $\pm 0.1\mu$ and a quadrant photodiode sensor detects particle position with resolution 15 nm at a 2 kHZ sampling rate. A fraction of the laser power is used to generate the optical trap: the optical trapping constant in the focal plane is, on average, $k \sim 1.7$ pN μm^{-1}, but is determined for each trapping plane location by analysis of the power spectral density. The maximum particle displacements in the focal plane are $\Delta x \sim 350$ nm or less than $1/10$ of the particle diameter.

The focal plane to which the colloid is tightly confined is positioned by raising or lowering the objective lens. The closest possible distance of the focal point from the solid surface is estimated from the defocusing of particle images and confirmed by fitting with predictions of $D_{\|}(z)$. When the focal point is closer than a particle radius from the solid interface (i.e., $z \leq a$), or alternatively within a particle radius of the upper water-oil or water-vapor interface (i.e., $z \geq z_{\mathrm{film}} - a$), the probe particle cannot track with the focal point. The optical trap does not have sufficient strength to pull the particle into the upper, high surface tension interface, nor into the solid, and consequently, the particle escapes from the trapping (focal) plane and appears defocused. Thus, by viewing the images of the probe particle we can judge where the trapping plane is located relative to the upper and lower interfaces. Near these interfaces, we sample the particle fluctuations in a sequence of planes that differ by $\Delta z = 1$ μm, or about $1/5$ of the particle diameter, and assign $z/a = 1$ to that trapping plane at the closest distance to the surface where the particle remains focussed and the z dependence of the measured $D_{\|}$ disappears. At each focal point location, z, we sample 200 sec of particle motion at 2 kHz and, using Eq. (1), fit $D_{\|}$ to the resulting PSD (Fig. 2). We also show results in Fig. 3 for $D_{\perp}$ near the solid surface, measured using orthogonal orientation of the solid surface.

Figure 3 is a composite of anisotropic mobility measurements for a silica particle in a thin water film sandwiched by the lower hydrophilic solid surface (right side of figure) and an upper water-oil or water-vapor interface (left side). Each point corresponds to a fitted value of $D_{\|,\perp}(z)/D_0$ from a single trajectory's PSD and the error in the fitted value as well as the overestimated error in z/a is within the

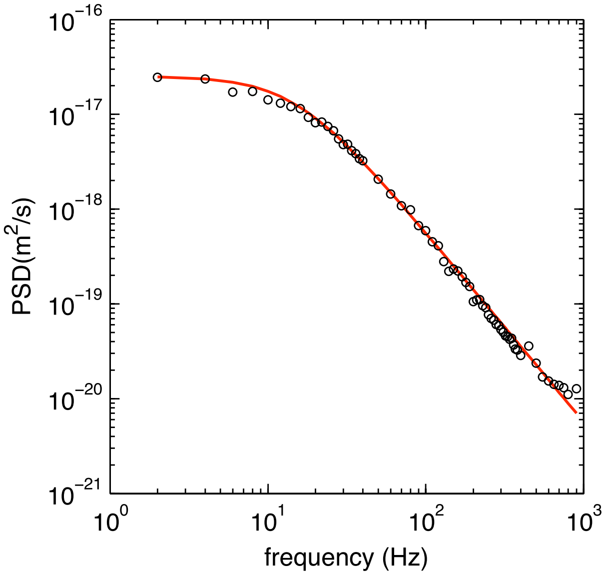

FIG. 2 (color online). A representative power spectrum density constructed from a 200 s trajectory of a single colloidal particle, sampled at 2 kHz at focal plane $z/a = 8$ above the solid surface. This experimental PSD data is fit to Eq. (1) using nonlinear regression and the fitted Lorentzian curve is included. The fitting parameters and associated error for this Lorentzian fit is $D_{\|} = (8.4 \pm 0.3) \times 10^{-14}$ m^2 s^{-1}. This small error in fitting the mobility is characteristic of all PSDs generated at each z/a. We overestimate the error in z/a as $1/2$ of our focal point step-size, or $\Delta z/a = \pm 0.20$.

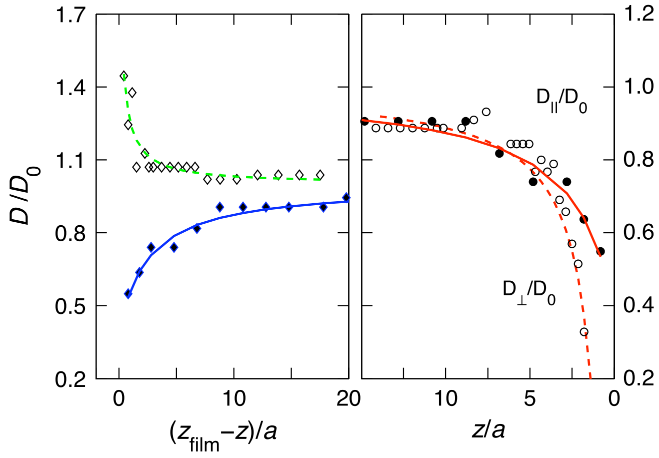

FIG. 3 (color online). Anisotropic mobility near fluid-fluid interfaces (left side) and solid surface (right side) versus distance from surface. Left: $D_{\|}/D_0$ versus dimensionless distance from fluid-fluid interface, $(z_{\mathrm{film}} - z)/a$, for water-vapor interface (open triangles) and water-oil interface (solid triangles). Lines are first order predictions of $D_{\|}/D_0$ for surfaces with perfect slip, $g_1^{\|} = +3/8$ (solid line), which compares with water-vapor interface, and for the no-slip surface, $g_1^{\|} = -9/16$, which compares with the oil-water interface. Right: $D_{\|}/D_0$ (filled circles) and $D_{\perp}/D_0$ (open circles) versus dimensionless distance from hydrophilic solid surface, z/a. Included for comparison is the first order hydrodynamic predictions for $g_1^{\|} = -9/16$ and $g_1^{\perp} = -9/8$.

size of the data points. When the particle is close to the solid surface ($1 \leq z/a < 10$) we measure both $D_{\|}/D_0$ (filled points) and $D_{\perp}/D_0$ (open points), and show that the hydrodynamic friction increases. These data are consistent with previous OT measurements [15] near no-slip solid surfaces (including hydrophobic solid surfaces) where both Brenner's exact result and Faxen's Law hold.

As the particle is elevated to the top of the water film of thickness z_{film}, it encounters the fluid interface, either a water-oil interface (solid triangles), or in a different experiment, the water-vapor interface (open triangles). Near the water-vapour interface, the mobility increases, or the friction decreases dramatically, reflecting the surface's inability to support a shear stress. These measured values of $D_{\|}/D_0$ for the water-vapor surface are consistent with theoretical predictions for mobility near surfaces which are perfectly slipping, or incapable of supporting a shear stress, also shown in Fig. 3. To first order in a/z, the classical prediction by Lee *et al.* [2] is

$$\frac{D_{\|}}{D_0} = 1 + \frac{3}{16}\left(\frac{2\eta_1 - 3\eta_2}{\eta_1 + \eta_2}\right)\left(\frac{a}{z}\right),$$

with η_1 being the viscosity of the fluid where the diffusing probe particle is located, and η_2 the viscosity of the other fluid. This prediction spans the slip and no-slip predictions: if $\eta_2 \longrightarrow \infty$, the parallel mobility decreases as if near a solid no-slip boundary while if $\eta_1 \gg \eta_2$, the parallel mobility is enhanced. In the case of the water-vapor interface, estimated at $\eta_1 = 1$ cP and $\eta_2 = 0.02$ cP respectively, recovering $g_1^{\|} = 0.36$, which is close to that of the perfect-slip boundary of $3/8 \sim 0.375$. On the other hand, the viscosity of the mineral oil is estimated at $\eta_2 \sim 34$ cP, leading to $g_1^{\|} = -0.54$ for the water-oil interface, close to the ideal no-slip value of $g_1^{\|} = -9/16 \sim 0.56$.

Using OT, we have measured for the first time, the friction of a particle near fluid-fluid interfaces, specifically a liquid-gas surface which does not support stress, and a liquid-liquid surface. We demonstrated the dramatically different behavior of the local mobility of a colloid particle when near these surfaces: near the water-vapor surface the particle's friction is diminished with respect to its bulk value while near a water-oil surface (as well as water-solid surfaces) the particle friction is enhanced. We envisage that this technique can be applied to various complex interfaces, including surfaces modified by surfactants and membranes.

---

*To whom all correspondence should be addressed. sevick@rsc.anu.edu.au

[1] H. Brenner, Chem. Eng. Sci. **16**, 242 (1961).
[2] S. H. Lee, R. S. Chadwick, and L. G. Leal, J. Fluid Mech. **93**, 705 (1979).
[3] S. H. Lee and L. G. Leal, J. Fluid Mech. **98**, 193 (1980).
[4] E. Lauga and T. M. Squires, Phys. Fluids **17**, 103102 (2005).
[5] T. Bickel, Phys. Rev. E **75**, 041403 (2007).
[6] C. Neto, D. R. Evans, E. Bonaccurso, H-J. Butt, and V. S. J. Craig, Rep. Prog. Phys. **68**, 2859 (2005).
[7] L. Bocquet and J.-L. Barrat, Soft Matter **3**, 685 (2007).
[8] C.-H. Choi and C.-J. Kim, Phys. Rev. Lett. **96**, 066001 (2006).
[9] H. Faxen, Ark. Mat. Astron. Fys. **17** (1923).
[10] L. Joy, C. Ybert, and L. Bocquet, Phys. Rev. Lett. **96**, 046101 (2006).
[11] P. Lancon, G. Batrouni, L. Lobry, and N. Ostrowsky, Europhys. Lett. **54**, 28 (2001).
[12] M. D. Carbajal-Tinoco, R. Lopez-Frenandez, and J. L. Arauz-Lara, Phys. Rev. Lett. **99**, 138303 (2007).
[13] B. Lin, J. Yu, and S. A. Rice, Phys. Rev. E **62**, 3909 (2000).
[14] S. Jeney, B. Lukic, J. A. Kraus, T. Franosch, and L. Forro, Phys. Rev. Lett. **100**, 240604 (2008).
[15] E. Shaffer, S. F. Norrelykke, and J. Howard, Langmuir **23**, 3654 (2007).
[16] G. M. Wang, E. M. Sevick, E. Mittag, D. J. Searles, and D. J. Evans, Phys. Rev. Lett. **89**, 050601 (2002).